Received: 23 December 2020 | Revised: 20 April 2021 | Accepted: 12 May 2021

DOI: 10.1002/er.7005

RESEARCH ARTICLE

INTERNATIONAL JOURNAL OF ENERGY RESEARCH WILEY

Thermocline vs. two-tank direct thermal storage system for concentrating solar power plants: A comparative techno-economic assessment

Mario Cascetta[1] | **Mario Petrollese**[1] | **Joseph Oyekale**[1,2] | **Giorgio Cau**[1]

[1]Department of Mechanical, Chemical and Materials Engineering, University of Cagliari, Cagliari, Italy

[2]Department of Mechanical Engineering, Federal University of Petroleum Resources, Effurun, Nigeria

Correspondence
Mario Petrollese, Department of Mechanical, Chemical and Materials Engineering, University of Cagliari, Via Marengo, 2, Cagliari, Sardegna 09123, Italy.
Email: petrollese@unica.it

Summary

This paper concerns the ongoing studies on a Concentrated Solar Power (CSP) plant in operation in Ottana (Italy), comprising a 629 kW organic Rankine cycle (ORC) unit fed by a linear Fresnel solar field. Hexamethyldisiloxane (MM) and "Therminol SP-I" are used respectively as ORC working fluid and heat transfer fluid in the solar receivers. A two-tank direct Thermal Energy Storage (TES) system is currently integrated in the CSP plant, serving as a direct interface between solar field and ORC. With the view of improving the solar facility, two alternative TES configurations were proposed in this study: a one-tank packed-bed TES system using silica as solid storage media and another similar one including encapsulated phase-change material (molten salt). Comprehensive mathematical models were developed for simulating daily behaviour as well as for assessing yearly performance of the various TES technologies. Furthermore, a preliminary economic analysis was carried out. Results showed poorer response of the one-tank TES system to large fluctuations in the ORC inlet fluid temperature, leading to reduction in the mean ORC efficiency (18.2% as against 19.7% obtained with the two-tank TES). Conversely, higher energy storage density and lower thermal losses were obtained adopting the one-tank TES, resulting in about 5% more annual solar energy yield. Invariably, equivalent annual ORC energy production of 0.92 GWh/year was obtained for the three TES configurations. Additionally, adopting a one-tank TES system meant that the purchase costs of a second tank and its storage medium (thermal oil) could be saved, resulting in investment costs about 45% lower and, ultimately, levelized cost of storage about 48% lower than what obtains in the two-tank TES system.

KEYWORDS

concentrating solar power, packed-bed, phase change materials, TES system, thermal storage medium

1 | INTRODUCTION

Although some controversies still exist regarding the capabilities of renewable energy systems to fully and sustainably satisfy global energy needs someday, the critical roles the renewables will play in the future energy mix are never in doubt. Main drivers of the universal consensus on the importance of renewable energy systems include the potential depletion of fossil fuels and, most importantly, their adverse effects on the environment.[1] Consequently, substantial efforts are in progress aimed at improving exploitation and conversion technologies of renewable energy resources. Solar energy, being one of such resources with universal availability and accessibility, is currently being practically exploited for electricity generation using the photovoltaic (PV) and concentrated solar power (CSP) technologies,[2] but also other applications, such as feeding air-conditioning systems,[3] heating water in thermal solar systems[4] and solar green houses,[5] are being explored towards efficient exploitation of this renewable source. While PV systems convert solar irradiation directly to electricity for immediate applications, they are limited in the use of solar energy in the thermal form.[6] Conversely, CSP technologies convert solar direct normal irradiation (DNI) to thermal energy at first, which can then be exploited either for direct heat application, or further processed for electricity generation via power cycles.[7,8] In this regard, definite research and practical efforts are being made over the years to further improve CSP systems, generally towards the advancement of clean and sustainable energy systems as viable alternatives to conventional systems.[9] The aforementioned developmental efforts notwithstanding, several impediments still retard the growth and practical deployment of CSP systems today, a situation that has placed a high premium on continued research activities in this field. Most CSP-based energy systems are characterized by low dispatchability and reliability, low efficiency and high conversion losses, high investment and running costs, complex control management strategies, amongst others.[10] These features emanate fundamentally from the transient nature of solar irradiation, due to seasonal and diurnal fluctuations. Specifically, it would be imperative to shut down a CSP plant when solar irradiation is unavailable or insufficient to operate the system, thereby increasing also the system down-time, whereas surplus solar energy is often wasted at other times when it exceeds the nominal value. Thus, if CSP systems would be operated optimally to play their intended roles in the sustainable energy infrastructure, the limiting challenges should be minimized. For this reason, CSP designs usually integrate thermal energy storage (TES) systems,[11-13] which serve to accumulate excess solar thermal energy during surplus times for deferred usage in times of insufficiency.[14] In addition, to mitigate the fluctuating effects of solar irradiation on CSP-based systems, TES systems also serve the purpose of increasing the proportion of solar energy being exploited, thereby maximising the overall investment.[15,16] However, the practical deployments of TES in real CSP plants often attract higher degrees of freedom for designers, with attendant reductions in economic efficiencies of the integrated systems. Thus, research activities are in progress towards optimal design/selection of TES systems for real CSP plants, and this also generally informed the relevance of the study being reported in this research article.

With respect to CSP applications, it is common to classify TES systems on the bases of integration concept to the CSP section (active or passive TES system, direct or indirect configuration) and the mode adopted for heat storage (sensible heat,[17] latent heat[18] or thermochemical[19]). A succinct review of TES for CSP applications revealed that majority of the currently installed plants adopt sensible and latent modes of thermal storage,[14,20] with direct or indirect integration configuration.[21] Two-tank type has been widely adopted in CSP systems under operation, while one-tank thermocline TES systems using solid media such as rock or phase change material (PCM) are drawing increasing attention for their higher energy storage density.[22,23] In such systems, a temperature gradient called thermocline separates a hot zone at the top of the bed from a cold zone at the bottom.[24] In addition, it is common to add cheap solid materials such as granite, quartzite, or silica particles, for enhancing the specific heat capacity and reducing the storage volume, and ultimately reducing the cost of heat-transfer fluid (HTF).[25]

Owing to the potentiality of thermocline TES system in terms of high energy storage density and relative low costs, numerous studies have been presented in literature for investigating the feasibility and reliability of such systems in CSP applications. In this regard, Bruch et al[26] carried out an experimental investigation in a thermocline TES system while thermal oil was used as HTF. Specifically, they investigated the effects of temperature difference during charge and discharge phases, as well as effects of mass flow rate and partial load on the dimensionless axial temperature profile. Results demonstrated the suitable behaviour of the thermocline TES system when integrated in a CSP plant, particularly regarding the robust and controllable nature exhibited. This is confirmed by further experimental and numerical investigations related to multiple charge/discharge cycles.[27] Also, the performance of a pilot scale dual-media thermocline TES system using a mixture of silica rock and sand as storage media and oil as HTF was experimentally investigated by Couturier et al.[28] The authors concluded that

the thermal behaviour after multiple charge/discharge cycles is independent of most operating parameters and depends mainly on the thermocline control strategy. Rodat et al[29] developed a dynamic model of a CSP plant composed by a Fresnel solar field with oil as HTF, an organic Rankine cycle (ORC) unit, and a dual-media thermocline TES system. The numerical results confirmed the robustness of the overall solar plant also in possible critical situations if reliable control strategies are implemented for the TES system. A validation of these results is given by experimental tests made on a 30 m^3 cylindrical tank equipped with thermocouples for temperature measurements at the inlet, the outlet, and the middle sections of the bed.[30] Chacartegui et al[31] investigated the expected performance of an ORC plant coupled with a 5 MW CSP plant of parabolic trough type and integrated with two different thermal storage types: a direct TES system using molten salt as both HTF and storage medium and an indirect one using diathermic oil as HTF and molten salt as storage medium. Results showed a similar efficiency of the power block comparing the two TES systems, but the direct TES system requires a tank volume reduced by 26% compared to the indirect TES. Moreover, techno-economic analyses were also presented in literature to demonstrate the profitability of thermocline TES configurations. A numerical comparison between two-tank and thermocline storage systems was carried out in Rodríguez et al[32] to evaluate the best system to integrate with a CSP-ORC system. The results revealed the superior global attractiveness of the thermocline solutions, since they exhibited similar thermal performance but at a much lower cost of about 30%. The relative cost reduction of TES systems based on thermocline configurations was also proven by Pacheco et al,[13] based on the experimental results carried out on a small pilot-scale (2.3 MWh) thermocline indirect storage system using molten salt as HTF.

Recently, innovative thermocline TES configurations based on a combination of solid media and PCM were proposed in literature for enhancing the thermal performance and thermal stability of these storage devices. On this subject, a new concept of thermocline-like TES device called multi-layered solid-PCM (MLSPCM) was presented in Galione et al.[33] Practically, the middle section of a packed bed is filled with cheap solid particles, while the top and bottom of the packed bed are respectively occupied by two types of encapsulated PCM close in phase change temperatures to the operating temperature limits.[34] In this case, effects of thermal buffering on PCM layers gave rise to only minor degradation of the thermocline in the entire charging cycle. Moreover, reducing the volume of the encapsulated PCM resulted in very similar storage quality, albeit at much higher costs than what obtains with the solid-filler material. Similarly, Zanganeh et al[35] presented a multi-layered TES system for CSP applications featuring a single thin PCM layer with elevated melting point positioned at the top of a packed bed of rocks. The simulations showed that stability would be sufficiently achieved for the outflow air temperature close to the melting point of the PCM, with PCM quantity measuring only about 1.33% of the total storage volume, without any negative effect on the overall efficiency.

All the above-cited studies clearly show that the choice of the most appropriate TES technology for practical applications remains daunting for designers and practitioners, due basically to the high dynamical tendencies during operations. In particular, different storage materials often possess different heat transfer characteristics, which could usually be enhanced depending on operating temperature range, thermal inertia, and HTF flow control; all of which correlate with the overall cost of TES systems. A research gap in this field remains the technical and economic evaluation of different TES types in real CSP plants with known operational features. The results of such comparative studies, if carried out comprehensively enough, would serve as viable sources of information for designers, policymakers, and other stakeholders, in the design/selection of appropriate TES technologies for future CSP projects.

In order to contribute substantially to the research gap identified in the foregoing, this study is aimed at comparative techno-economic assessment of different TES technologies prominent for application in medium-scale CSP systems, with reference to a real 629 kW CSP-ORC plant running at Ottana, Italy. The plant integrates an active direct two-tank TES system using thermal oil as storage medium. Currently, research activities are underway to investigate practical solutions for improving the entire facility, of which structural optimization of the installed TES technology is vital. Thus, other similar TES technologies are being considered that could provide better alternatives to the existing one. Specifically, the technical and economic performance of two other TES configurations, a one-tank thermocline packed-bed system with rock and sand as storage media and a similar one that incorporates PCM in form of capsules, are further investigated in comparison with the two-tank TES currently in operation. One of the most important issues addressed in this study is the interaction between the new proposed TES system with the solar field and the ORC plant currently installed. Adopting the two-tank system, both solar and ORC plants always work in a quite stable condition, since both the cold oil entering the solar field and the hot oil entering the ORC plant keep generally an almost constant temperature, therefore the

circulating mass flow rate in the solar field is regulated only according to the DNI to keep constant the outlet temperature. Conversely, using the thermocline TES system, the solar field is expected to receive oil at increasing temperature, particularly when the TES system is near the end of the charge phase. In this case, the mass flow rate needs to be increased to meet the requested oil temperature at the exit. In addition, the ORC plant is expected to receive oil at lowering temperature from the TES system during the discharge phase. Ultimately, both the solar field and the ORC plant are expected to work partially in off-design conditions and this aspect is carefully investigated in this work, since it affects the global efficiency of the plant. Moreover, the current ORC plant is one of the largest in size integrated with a CSP plant and a TES system completely operating at the moment, making this study more attractive. A dynamic simulation is a credible choice to reproduce the behaviour of the overall plant as close as possible to the reality, also evidencing the effects on performances by adding a layer of PCM at the top of the bed of the TES system. As aforementioned, findings from such comparative study would be directly applicable to other medium-scale CSP systems, thereby providing a general scientific contribution that would be useful to designers, researchers as well as energy policymakers. The study is particularly vital, given that one of the compared TES configurations, the thermocline TES configuration that combines solid material with PCM as storage media, is relatively new, and thus requires more investigations regarding its practical performance in real power plants as is the case here.

The specific objectives of this paper are:

- Detailed thermodynamic modelling of the three TES systems as well as the CSP and ORC units.
- In-depth analyses of daily control management strategies of the different TES technologies for integration with the CSP and ORC units.
- Comparative annual energy performance of the plant with respect to the different TES technologies.
- Comparative economic performance of the TES technologies based on levelized cost of storage.

2 | PLANT CONFIGURATION

2.1 | Current configuration

As mentioned above, a real medium-scale CSP plant running at Ottana (Italy)[36] is considered as case study. At present, this solar facility integrates as a vital sub-system, a two-tank direct TES unit for accumulating the solar thermal energy produced in the solar field. At nominal conditions, the storage system can store about 15 MWh of thermal energy, accumulating around 195 tons of thermal oil ("Therminol SP-I"). The latter flows through the solar field as HTF and serves equally as storage medium in TES tanks. The solar field is designed for a total collecting area of about 8400 m^2, composed specifically of six parallel lines of linear Fresnel collectors with tracking mechanism along North-South direction. The HTF circulating through the solar field is designed for a mass flow rate of 18 kg/s and a temperature difference of 110°C between outlet and inlet collector sides. The control system is set to regulate HTF mass flow rate as solar irradiation fluctuates, to maintain as constant the HTF nominal temperature at solar collector exit. At power generation phase, the thermal oil stored in the TES hot tank is pumped to the power block, where its energy content is exploited as it flows through the interfacing heat exchangers, after which it is pumped back to the TES cold tank. An ORC unit ("Turboden 6HR Special") based on regenerative Rankine cycle running with organic working fluid (hexamethyldisiloxane, $C_6H_{18}OSi_2$). is used for thermal-to-electricity thermodynamic conversion process.

2.2 | Alternative TES configurations

In this work, the actual two-tank TES system is compared with two alternative TES configurations. A one-tank thermocline packed-bed system using rock and sand as thermal storage media is assessed vis-a-vis another similar but with the upper layer composed of capsules filled with PCM and sand in the interstices between the capsules. The adoption of PCM placed at the top of the tank is aimed at keeping as stable as possible the temperature of the oil supplied to the ORC unit for improving the performance of the overall system.[35] In both cases, a reservoir with the same dimensions of the hot tank present at the facility is adopted, consisting in a cylindrical steel tank of 11 m in diameter and 3.5 m in height.

Figure 1 shows the system concept of the overall CSP plant as well as the three TES configurations compared in this study. In the case of the one-tank packed-bed system, during the charging phase, the hot HTF enters from the top of the tank and releases the heat to the solid media or PCM, charging the TES system and generating a thermocline along the axis of the bed. Conversely, during the discharging phase, the cold thermal oil enters from the bottom of the tank in reversed flow, absorbs the heat from the solid media or PCM, and exits from the top.

Table 1 reports the thermal properties of the various storage media considered in this study. In the packed-bed

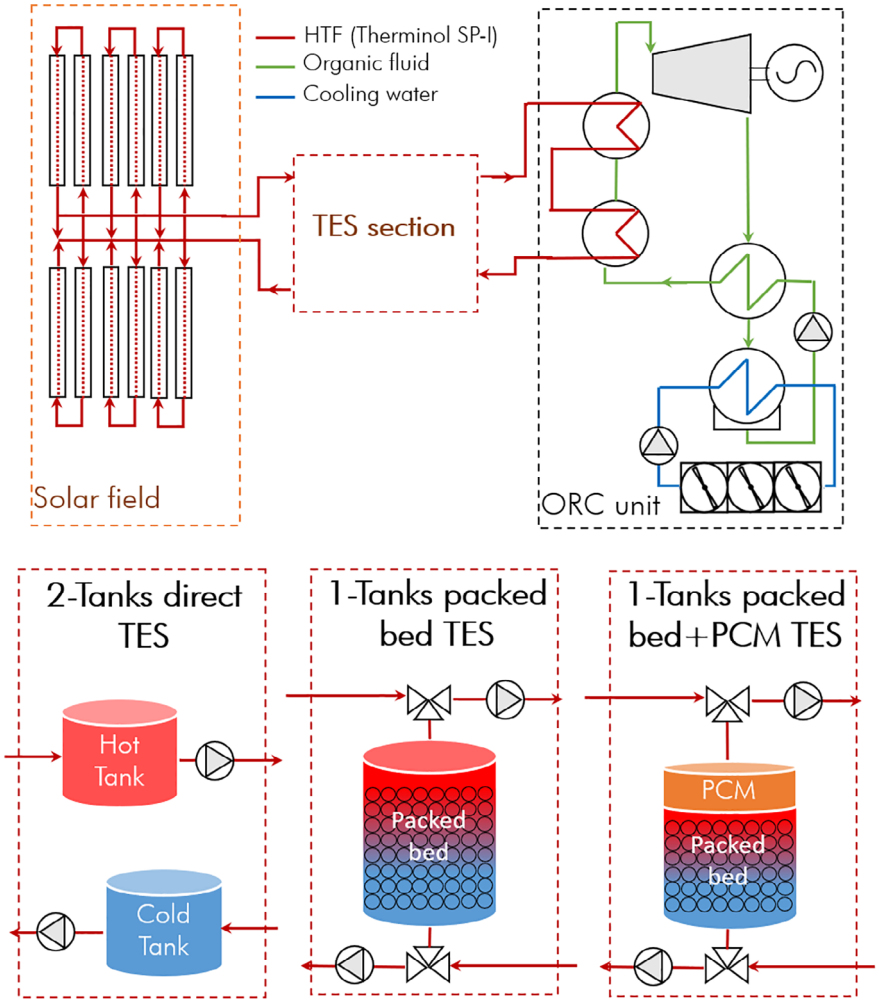

FIGURE 1 Schematic of the CSP plant including the three TES configurations compared in this study

TABLE 1 Thermal and physical properties of the storing media at 260°C[a]

	OIL[a]	SILICA	PCM	SHELL
Density kg/m^3	704	2500	1950	7900
Latent heat [kJ/kg]	-	-	161	-
Specific heat capacity J/(kg K)	2755	830	1480	500
Volumetric heat capacity kJ/(m^3 K)	1940	2075	2886	3950
Thermal conductivity W/(m·K)	0.10	0.10	0.48	15

[a]The thermal properties of the oil are temperature-dependent, while the silica and PCM properties can be considered as constant in the operative range of temperature observed in the TES system.

case, silica is used as solid storage medium due to its low specific costs and the large range of operating conditions this material can operate without large variations in its thermal properties. According to Bruch et al,[27] a mix of rock and sand with a distribution of 80% and 20% is chosen to reduce the bed void fraction of the packed bed. The diameter of rock and sand are set to 30 mm and 3 mm respectively. In the solid + PCM case, the 90% in volume of the TES is constituted by silica rock and sand as in the previous case, while PCM capsules having a diameter of 25 mm and a shell made of steel with a thickness of 1 mm are placed at the top of the bed. The void between the capsules is filled with sand. The PCM is made of molten salt (KNO_3 60% + $NaNO_3$ 40%) and it has a melting temperature of 221°C. This choice was made for technical reasons since the melting point temperature is the minimum acceptable temperature to avoid substantial degradation in the ORC performance (this effect will be analysed in Section 3.3), but also because it is a proven and commercially available medium commonly used in CSP systems. Both beds with and without PCM have a

porosity set to 0.27, while for the capsules, filling coefficient was taken as 0.85, to make room for fluid expansion when undergoing the melting process.

Based on storage media characteristics and current vessel volume (330 m^3), the maximum storage capacities of the three alternative TES configurations are determined and highlighted below (Table 2). By considering the current two-tank TES configuration as reference, an increase of about 45% and 55% in the maximum storable energy is determined for the packed-bed and packed-bed + PCM systems, respectively. Furthermore, substantial reduction in the mass of oil used as storage medium (about 65%) is observed in the one-tank alternatives, with a significant consequence in the cost-effectiveness of the TES system.

3 | MATHEMATICAL MODELS

This section introduces the mathematical models developed in MATLAB-SIMULINK for the simulation of the three TES configurations compared in this study, as well as the other units of the CSP-ORC plant. Thermal properties of the HTF declared by manufacturer[37] are taken as reference, while the main design assumptions are reported in Table 3.

3.1 | Fresnel solar field

The performance of the solar field (Fresnel type) mainly depends on some environmental parameters, such as the available DNI, solar azimuth, ambient temperature, and wind speed. According to Cocco et al,[38] the solar thermal power input into the receiver $(\dot{Q}_{INC})$ is given by the product of the solar field collecting area A_{SF}, the reference optical efficiency $\eta_{OPT,R}$, the Incidence Angle Modifier (IAM), the end-loss optical efficiency (η_{END}) and the surface cleanliness efficiency η_{CLN}, as:

$$\dot{Q}_{REC} = DNI \cdot A_{SF} \cdot \eta_{OPT,R} \cdot IAM \cdot \eta_{END} \cdot \eta_{CLN} \quad (1)$$

The Incidence Angle Modifier, calculated as product of the longitudinal (IAM_L) and transversal (IAM_T) components, is determined as a polynomial function of the longitudinal and transversal components θ_L and θ_T of the solar incidence angle:

$$IAM_L = 1.004 - 1.311 \cdot 10^{-2}\theta_L + 3.471 \cdot 10^{-4}\theta_L^2 - 8.860 \cdot 10^{-6}\theta_L^3 + 5.822 \cdot 10^{-8}\theta_L^4 \quad (2)$$

$$IAM_T = 0.9942 + 1.23 \cdot 10^{-3}\theta_T - 4.659 \cdot 10^{-4}\theta_T^2 + 1.998 \cdot 10^{-5}\theta_T^3 - 3.242 \cdot 10^{-7}\theta_T^4 + 1.586 \cdot 10^{-9}\theta_T^5 \quad (3)$$

TABLE 2 Mass of solid or liquid media used to store energy and maximum energy stored for each case

Case	Two-tank system	One-tank Thermocline system (Rock + Sand)	One-tank Thermocline (Rock + Sand + PCM)
Mass of oil (t)	195	67	63
Mass of rock + sand (t)	-	607	557
Mass of PCM (t)	-	-	33
Maximum storable energy (MWh)	15.20	21.93	23.41

TABLE 3 Main design parameters introduced in the mathematical models

Solar field		TES system	
Net solar field area (A_{SF})	8400 m^2	Tank volume	330 m^3
Reference optical efficiency ($\eta_{OPT,R}$)	65.5%	Inner Tank diameter	11 m
Focal length (F)	4.97 m	Aspect ratio	0.32
Collector length (L_C)	99.45 m	Void fraction (*packed bed*)	0.27
Cleanliness efficiency (η_{CLN})	98%	Particle rock diameter (*packed bed*)	25 mm
Receiver volume (V_{REC})	1.20 m^3	PCM capsules diameter (*packed bed*)	25 mm
		Shell capsules thickness (*packed bed*)	1 mm

The end-loss optical efficiency was evaluated as a function of the longitudinal component of the incident angle, the collector length (L_C) and the focal height (F):

$$\eta_{END} = 1 - \frac{F}{L_C}\tan\theta_L \tag{4}$$

The HTF outlet temperature ($T_{HTF_{SF,O}}$) was determined by using the following energy balance of the receiver:

$$\rho_{HTF} c_{HTF} V_{REC} \partial \frac{T_{HTF_{SF,O}}}{\partial t} = \dot{m}_{HTF_{SF}} c_{HTF} \left(T_{HTF_{SF,O}} - T_{HTF_{SF,I}}\right) - \left(\dot{Q}_{INC} - \dot{Q}_{REC,L}\right) \tag{5}$$

where ρ_{HTF} and c_{HTF} represent the density and the specific heat of the HTF, V_{REC} the oil volume inside the receiver tubes while the overall receiver thermal losses, ($\dot{Q}_{REC,L}$), was evaluated as reported in Forristall.[39] Consequently, the mass flow rate circulating in the solar field ($\dot{m}_{HTF,SF}$) was set to obtain an exit temperature ($T_{HTF_{SF,O}}$) as close as possible to design value (260°C), taking as starting point the inlet HTF temperature ($T_{HTF_{SF,I}}$). The HTF circulating in the solar field ranges between a minimum of about 6 kg/s and a maximum of 18 kg/s, based on the pump characteristics. Moreover, according to the solar field control system implemented in the solar facility of Ottana, a DNI higher than 200 W/m^2 was imposed to activate the solar field thermal production.

3.2 | Thermal energy storage system

Owing to the different physical behaviour of the packed-bed TES configurations compared to the existing two-tank direct storage, two different mathematical models were developed for the comparative analysis. For both configurations, the overall thermal losses due to an imperfect insulation of the tank were evaluated considering an overall heat transfer coefficient (U_{TES}) of 0.3 W/m^{2}K.[40]

3.2.1 | Two-tank direct TES

According to Petrollese and Cocco,[41] a zero-dimensional modelling (namely, negligible thermal stratifications inside the tanks) based on mass and energy balances applied to the hot tank (HT) and cold tank (CT) was adopted for simulating the two-tank TES configuration:

$$\frac{\partial m_{HT}}{\partial t} = \dot{m}_{HTF_{SF}} - \dot{m}_{HTF_{ORC}} \tag{6}$$

$$\frac{\partial m_{HT} h_{HT}}{\partial t} = \dot{m}_{HTF_{SF}} h_{HTF_{SF,O}} - \dot{m}_{HTF_{ORC}} h_{HT} - U_{TES} A_{TES} (T_{HT} - T_{AMB}) \tag{7}$$

$$\frac{\partial m_{CT}}{\partial t} = \dot{m}_{HTF_{ORC}} - \dot{m}_{HTF_{SF}} \tag{8}$$

$$\frac{\partial m_{CT} h_{CT}}{\partial t} = \dot{m}_{HTF_{ORC}} h_{HTF_{ORC,O}} - \dot{m}_{HTF_{SF}} h_{CT} - U_{TES} A_{TES} (T_{CT} - T_{AMB}) \tag{9}$$

where m_{HT} and h_{HT} represent the HTF mass stored and mean enthalpy in the hot tank respectively, m_{CT} and h_{CT} the HTF mass stored and mean enthalpy in the cold tank, $\dot{m}_{HTF_{ORC}}$ the HTF mass flow rate sent to the ORC, $h_{HTF_{ORC,O}}$ the HTF enthalpy at the outlet side of the ORC unit and A_{TES} the tank external area.

3.2.2 | One-tank packed-bed TES

A transient, one-dimensional (1-D), two-equation numerical model was employed for evaluating the thermal behaviour of the packed-bed TES system. The temperatures of the HTF (T_{HTF}) and the solid media or PCM (T_{BED}) were calculated separately, considering a 1-D axisymmetric geometry with a spatial step of 0.01 m and a time step of 10 s, and assuming a constant temperature profile in the radial direction. According to Bruch et al,[26] a weighted average diameter of 25 mm is considered for the silica. The following equations refer to the energy balance applied to HTF and to the silica or PCM (BED), respectively[26]:

$$\varepsilon(\rho c)_{HTF} \frac{\partial T_{HTF}}{\partial t} + (\rho c)_{HTF} u \frac{\partial T_{HTF}}{\partial x} = \varepsilon k_{eff} \frac{\partial T_{HTF}}{\partial x^2} + \alpha A_{BED} (T_{BED} - T_{HTF}) - U_{TES} A_{TANK} \left(\overline{T}_{HTF} - T_{AMB}\right) \tag{10}$$

$$(1-\varepsilon)(\rho c)_{BED} \frac{\partial T_{BED}}{\partial t} = \alpha A_S (T_{HTF} - T_{BED}) \tag{11}$$

where ε represents the bed void fraction, k_{eff} the effective thermal conductivity of the overall bed, α the convective heat transfer coefficient, A_{BED} and A_{TANK} the superficial area per unit of volume of the bed and of the tank, respectively, calculated according to previous studies.[42,43] The convective heat transfer coefficient α is mainly a

function of the Nusselt number according the following known correlation,[44] while A_S depends on the particle diameter and void fraction:

$$Nu = 2.0 + 1.1 \cdot Re_p^{0.6} \cdot Pr^{0.33} \quad (12)$$

$$A_S = \frac{6 \cdot (1-\epsilon)}{d_p} \quad (13)$$

Considering that the thermal conductivity of the PCM is low and the diameter of the capsules is relatively larger in this case,[45] effect of Biot number is not negligible, and thus it was considered in the model. In the third case, the storing media at the top of the bed is a mixture of PCM inside capsules, the shell of the capsules and sand. The sum of the weights of the three media is equal to the complementary of the global void coefficient equal to 0.27 while the volumetric heat capacity is given by the weight average between the three media:

$$(\rho c)_{Top_{Layer}} = 0.38 \cdot \rho_{PCM}[c_{PCM} + L_{PCM} \cdot D(T_{PCM})] + 0.13 \cdot \rho_{sand} c_{sand} + 0.22 \cdot \rho_{Shell} c_{shell} \quad (14)$$

where L_{PCM} is the latent heat of fusion of PCM while $D(T_{PCM})$ is a function that accounts for the latent heat of fusion absorbed during the melting process:

$$D(T_{PCM}) = 4 \cdot \exp\left\{ -\left[\frac{4(T_{PCM} - T_{PCM,m})}{(T_{PCM,l} - T_{PCM,s})}\right]^2 \right\} \cdot \left[(T_{PCM,l} - T_{PCM,s}) \cdot \sqrt{\pi}\right]^{-1} \quad (15)$$

It can be observed that the value of $D(T_{PCM})$ would be equivalent to zero at every point, safe at the interval between the liquid phase temperature ($T_{PCM,l}$) and solid phase temperature ($T_{PCM,s}$), where $T_{PCM,m}$ is the average value. Also, in order to ascertain the energy balance through the phase transition by the multiple of $D(T_{PCM})$ and L_{PCM}, integrating $D(T_{PCM})$ over the range of all temperatures gives 1. Lastly, the highest value is obtained when the temperature equals $T_{PCM,m}$. This function enhances the phase change process, close to what obtains in practice, in comparison with the enthalpy model.

The effective thermal conductivity, k_{eff}, of the bed takes into account both the silica/PCM and HTF conductivity given by the following correlations:

$$k_{eff} = k_l \frac{1 + 2\beta\phi + (2\beta^3 + 0.1\beta)\phi^2 + \phi^3 0.05\exp(4.5\beta)}{1 - \beta\phi} \quad (16)$$

$$\phi = 1 - \varepsilon\,\beta = (k_s - k_l)/(k_s + 2k_l) \quad (17)$$

where k_s and k_l represent thermal conductivity of the solid media (PCM or rock) and of oil, respectively.

3.3 | Organic Rankine cycle unit

Performance of the ORC plant was evaluated by determining the net power and the outlet temperature of the HTF exiting the power block, depending on the HTF mass flow rate and temperature at ORC inlet, as well as inlet temperature of the heat sink (water, with mass flow rate assumed constant and equal to the nominal value). The experimentally validated mathematical model proposed in Petrollese et al[46] was used for predicting performance of the power block. Figure 2A shows how the net power produced by the ORC unit responds by varying temperature and mass flow rate of the HTF entering the ORC, with a cooling water temperature at inlet side of the condenser kept constant at 35°C. The effect of feeding the ORC unit with a reduced mass flow rate and a lower HTF inlet temperature is shown, with an obvious degradation in the power block performance as the thermal input reduces. Similarly, Figure 2B depicts how the net power responds to an increase in temperature of the inlet cooling water, assuming that the design thermal power is constantly supplied to the ORC. Even in this case, a degradation of the ORC performance is observed, caused chiefly by the increase in saturation pressure during the condensation process.

Finally, due to the transient nature of solar energy, it is anticipated that the ORC unit would require daily start-up and shut down. Since the energy input required during the start-up phase is not negligible, on the basis of Ottana solar facility experience, it was assumed that 30 minutes are needed for the power plant to complete its start-up and during this period the power block is fed by a design thermal power input without producing any electrical power.

3.4 | Plant management

The DNI and state-of-charge of the TES system are the two main parameters employed in the plant management, leading specifically to the following four operating modes:

- *Solar-to-TES*. The ORC unit is kept off and the TES system is charged by the HTF exiting the solar field to reach the TES full-charge condition. In the case of a two-tank direct storage, the hot tank accumulates hot oil exiting the solar field, while the cold oil

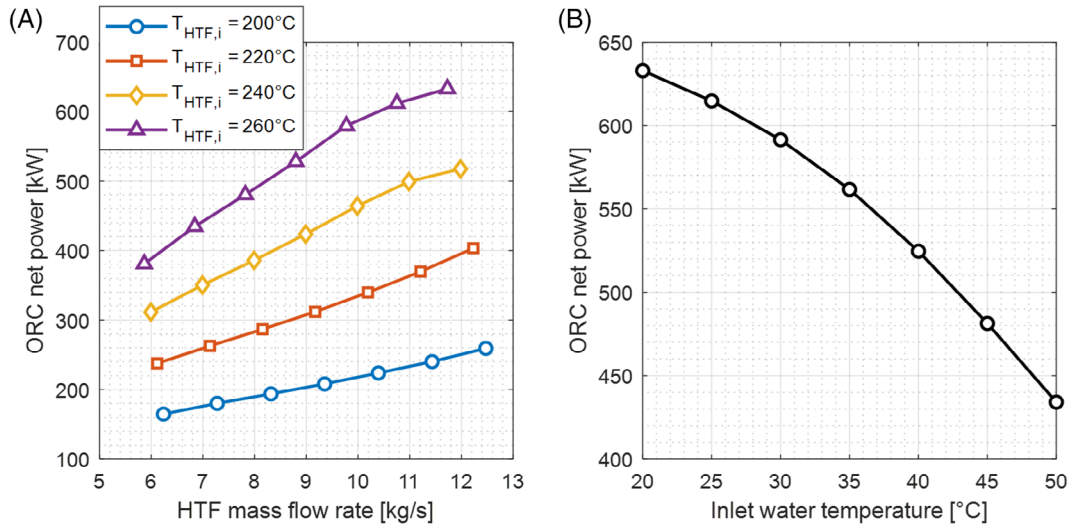

FIGURE 2 Responses of ORC net power by varying, A, mass flow rate and inlet temperature of HTF, B, water temperature at condenser inlet

accumulated in the cold tank feeds the solar field. This operating mode is active until all the thermal oil is transferred to the hot tank. For the one-tank TES systems, the bed temperature increases gradually with inflow of hot HTF from solar field, and the HTF leaving the tank from the bottom returns to the solar field. With the rise in the average temperature of the packed bed, an increase in the thermal oil leaving the tank occurs. Consequently, the rotational speed of the solar field circulation pump is adjusted to keep the outlet oil temperature close to the set value raising the HTF mass flow rate. This operation mode remains active until the pump reaches its maximum speed and the ORC is then switched on, since this condition is verified when the TES can be considered charged.

- *Solar-to-ORC + TES*. The operational ORC unit is set to the nominal electrical power value (629 kW net). The HTF mass flow rate feeding the turbogenerator is adjusted by means of a variable speed pump while the HTF circulating in the solar field exceeds the thermal power demanded by the turbogenerator. Consequently, the excess is stored in the TES section. The cold oil exiting the ORC is sent to the cold tank (two-tank case) or mixed with the thermal oil leaving the TES system and sent back to the solar field (one-tank case).
- *Solar + TES-to-ORC*. The mass flow rate of inlet HTF required for ORC operation at design conditions would not be sufficiently satisfied by the hot solar field HTF. Therefore, the TES system is discharged to make up for disparity in the thermal energy required for the ORC to operate at nominal conditions.
- *TES-to-ORC*. The solar field does not produce thermal energy and the ORC plant is exclusively fed by the TES system until the latter is completely discharged. Complete discharge occurs when all the thermal oil is stored in the cold tank for the case of two-tank direct storage or when the temperature of the HTF feeding the ORC is lower than 200°C, which is considered as the minimum acceptable by the ORC unit.

4 | RESULTS AND DISCUSSION

The expected performance of the CSP plant with different TES configurations is presented and analysed in this section. To begin with, the plant performance is reported for a typical summer day (day 240) characterized by clear sky conditions, chosen such that, starting from a completely discharged TES, all the operating modes mentioned above occur during the day. Next, the yearly performance to be expected of the plant is analysed.

4.1 | Daily performance

On the specified summer day chosen for analysis, the simulation results for the case of one-tank thermocline packed-bed system filled with rock and sand are shown in Figure 3. As can be seen, the HTF mass flow rate (Figure 3A) circulates in the solar field for almost 12 hours (from 5.30 AM to 5.30 PM). Since the solar field control system is set to maintain the exit temperature of the HTF at the design value, as much as possible, a variation of the mass flow rate with the solar radiation occurs. In the first part of the day, the Solar-to-TES operating mode is active and all the HTF heated up in the solar field is used to charge the TES system. For this reason, as

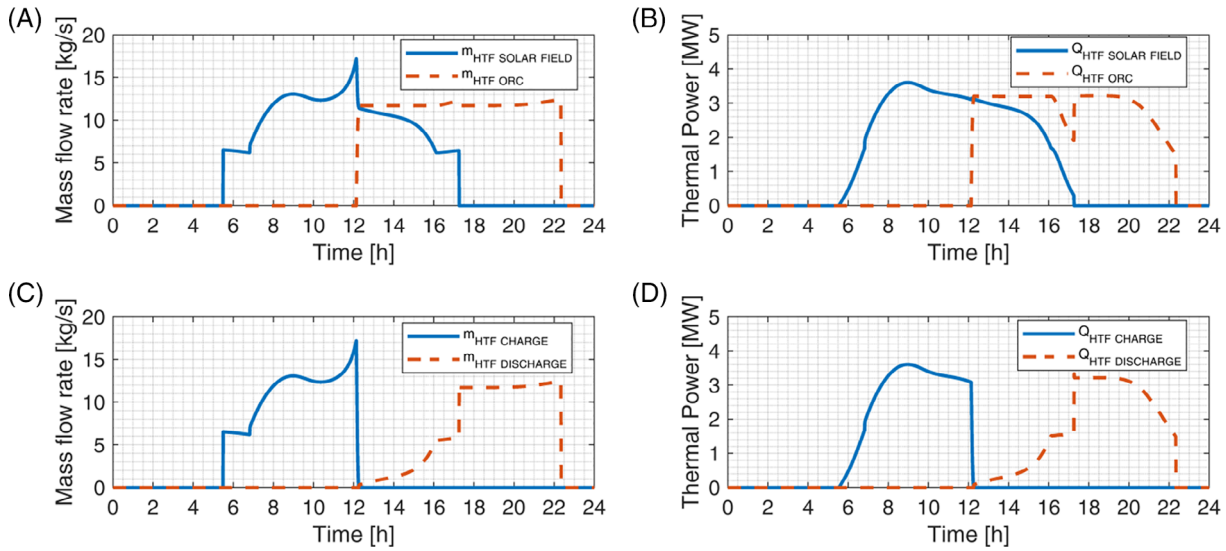

FIGURE 3 A, HTF mass flow rates and, B, correlated thermal power flows produced by the solar field and required by the ORC unit, C, consequent HTF mass flow rates and, D, correlated thermal power flows obtained during the charging and discharging phase of the TES system on a given summer day

shown in Figure 3C, the HTF mass flow rate sent to TES unit has the same trend of the mass flow rate coming from the solar field. The TES system is fully charged after about 7 hours (at about 12:30 PM). This condition can be observed through the quick increase of the rate of mass flow of the HTF through the solar field up to almost 18 kg/s (the maximum value allowable in the solar field), when the TES is approaching its full charge state. According to the implemented operating modes, the ORC unit is then started. Apart from a short period, when the thermal energy produced in the solar field goes beyond the thermal demand of the turbogenerator and the share of the solar field HTF mass flow is sent to the TES section (Solar to TES + ORC), the operating mode Solar + TES-to-ORC is active during the last part of the daytime. In fact, the solar field is unable to guarantee the thermal power requested by the ORC unit and the storage system is therefore discharged to make up the energy deficit, as shown in Figure 3C. This operating condition remains active up to about 5 PM, when the solar field is deactivated and only the TES system supplies the ORC plant (TES-to-ORC). This operating condition ends when the TES system is substantially discharged, namely when the temperature of the oil supplied by the hot tank drops to 200°C, taken as the minimum acceptable temperature by the ORC.

As shown in Figure 3B, the thermal power produced by the solar field follows a similar trend of the HTF mass flow rate apart from periods in which the temperature variations from their nominal values become predominant. This occurrence can be observed close to the start-up and shutdown of the solar field and when the TES is approaching its full-charge state. In this case, a significant rise in the HTF mass flow rate is not reflected in the thermal power due to a corresponding reduction in temperature difference between solar field inlet and outlet sides. Furthermore, the HTF temperature decrease during the last discharging period leads to a reduced thermal power input into the ORC plant (at constant HTF mass flow rate) and, consequently, to a decrease in the electrical power produced. As already observed for the mass flow rates, during the morning the trend of the thermal energy flowing into the storage system for charging overlaps the solar field thermal power curve. Similarly, when the TES-to-ORC mode is activated, the thermal power feeding the ORC unit coincides with the thermal power discharged by the TES section.

To further explain the phenomena occurring during the charge and discharge phase of the packed-bed system, Figure 4 highlights how the temperature profile of both solid media and oil evolve over time while charging (Figure 4A) and discharging (Figure 4B). The initial profile represents the thermal condition of the TES system at midnight as residual condition of the previous day. Up to 6 AM, the TES system is inactive and both thermal losses towards the external ambient and the thermal conductivity within the bed slightly modify the shape of the thermocline. When the charge phase begins, the hot oil enters from the top of the bed, and layers of the bed gradually increase their temperature beginning from the top up to a maximum of about 260°C. When the TES system is fully charged, in accordance with the plant management, the temperature of the bottom layer of the bed reaches about 200°C. At about 12:30 PM, the flow

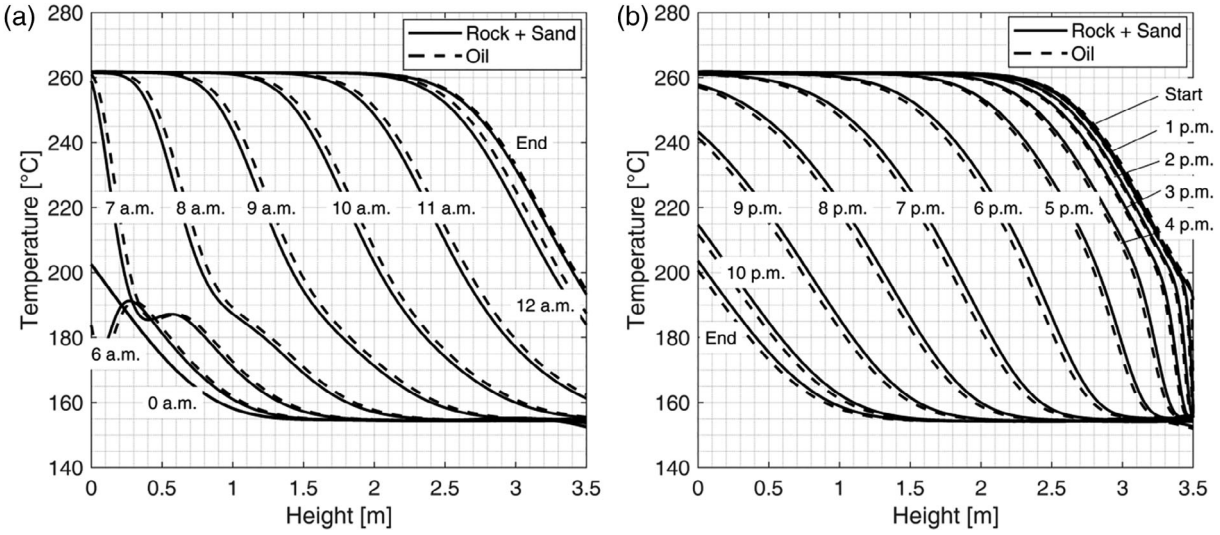

FIGURE 4 Evolution of the thermocline profiles over time during, A, the charge phase and, B, discharge phase, using rock and sand as solid media

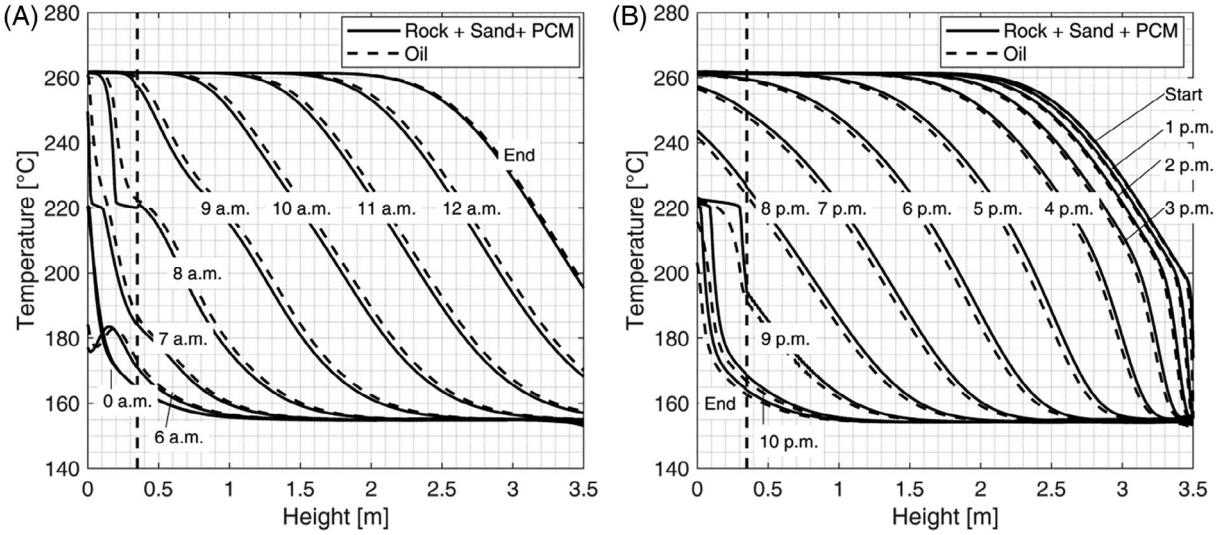

FIGURE 5 Transient evolution of the thermocline profiles during, A, the charge phase and, B, discharge phase using rock, sand and PCM as solid media

reverses, and the TES starts to discharge accumulated energy. During the first part of the discharge phase (Figure 4B), the overall system is in the "Solar + TES to ORC" operating mode, since the HTF flowing through the TES system must compensate the lacking mass flow rate needed to reach a nominal value of about 12 kg/s requested by the ORC plant. After 5 PM, the solar field becomes inoperative, therefore, only the TES system feeds the ORC plant, ("TES to ORC" operating mode). The discharge phase lasts for about 9 hours and almost all the bed reaches gradually the minimum value of about 155°C, except in the last layer at the top where the temperature remains higher. Indeed, this phase completes when the heated oil exiting the top of the tank attains a temperature still acceptable for the ORC unit to operate in an efficient way (200°C).

The substitution of a layer of the bed made by rock and sand with PCM capsules at the top of the bed is then investigated as a viable alternative. The height of the PCM layer has been assumed equal to 10% of the overall bed height. In Figure 5, a vertical dashed line placed at 0.35 m along the x-axis divides the bed into two zones. The zone at the left of the dashed line represents the side of the bed with PCM + sand, while the other to the right is the zone with rock and sand. Obviously, the inclusion of the PCM layer introduces a significant difference in

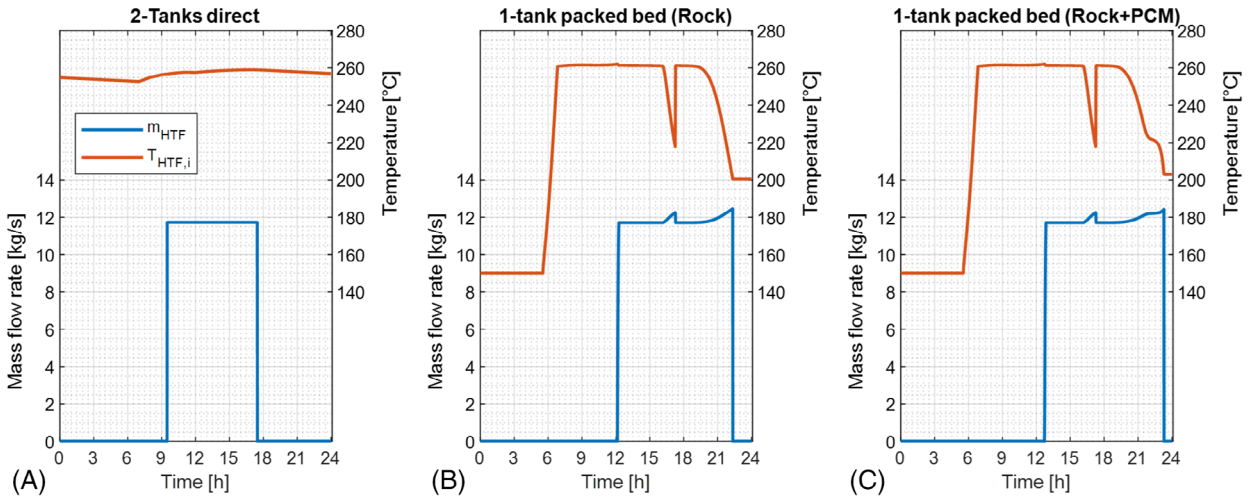

FIGURE 6 Mass flow rate and temperature of the ORC inlet HTF for, A, the two-tank direct TES configuration, B, the one-tank packed-bed filled with rock and sand and, C, the one-tank packed-bed with the addition of a PCM layer at the top of the tank

the evolution of the thermocline, compared with that obtained in the previous case. By referring to Figure 5A, the PCM capsules in the first part of the charge phase are heated by the HTF and their temperature increases until reaching the melting temperature (221°C). During melting, the temperature of PCM increases very slowly due to the latent heat of fusion, generating a step within the bed. Once the PCM is completely melted, the temperature increases faster, and the profile of the thermocline returns to be similar to that already shown in the case without PCM. During the discharge phase, the effect of introducing a PCM layer becomes evident when the TES is almost completely discharged and the PCM reaches its melting temperature (221°C). Analogously to the charge phase, the temperature remains almost constant during the solidification process, therefore the HTF temperature calculated at the outlet section of the tank decreases more slowly, thereby mitigating the drop in ORC performance due to low HTF inlet temperature.

4.1.1 | Comparison with the current TES configuration (two-tank)

Behaviour of the three different TES configurations (namely, the current two-tank direct storage, one-tank packed-bed filled with rock and sand and the latter topped with additional PCM layer) were compared with respect to the conditions on the chosen day. Mass flow rate and temperature of the ORC inlet HTF were the main performance variables considered for this analysis, reflecting respectively the quantity and quality of the thermal energy ready for supply into the ORC plant.

Figure 6 shows the main trends obtained for the two performance variables during the considered day for the three TES configurations analysed. For the same volume of the tank, the higher energy capacity introduced with the packed-bed configurations results in an increase in the continuous operating hours of the ORC unit. Another considerable effect in using packed-bed configurations is related to the ability to shift the ORC production towards night-time: in Figure 6 it is possible to observe the start-up phase postponed by about 2 hours for the one-tank configuration relative to the two-tank alternative and the ORC is in operation until midnight. Consequently, the ORC unit generally operates with lower ambient temperatures. This fact is beneficial to the ORC conversion efficiency, since dry coolers can reduce the inlet temperature of cooling water with a consequent reduction in the condenser pressure. On the other hand, significant variations in the delivered temperature occur in one-tank configurations due to the intrinsic characteristics of the packed-bed to store a medium at different temperature, unlike the use of a dedicated tank for storing the hot oil as in the two-tank configuration. Consequently, decrease in the ORC net power occurs for the one-tank configurations, especially towards the night-time, when the TES systems are approaching full discharge. The introduction of a PCM layer only mitigates this performance drop and its effect becomes evident for almost 1 hour. On the other hand, a limited temperature variation, mainly due to imperfect insulation of the hot tank, is observed by considering the two-tank case. Accordingly, the ORC unit can operate close to its nominal condition with marginal variations in the conversion efficiency.

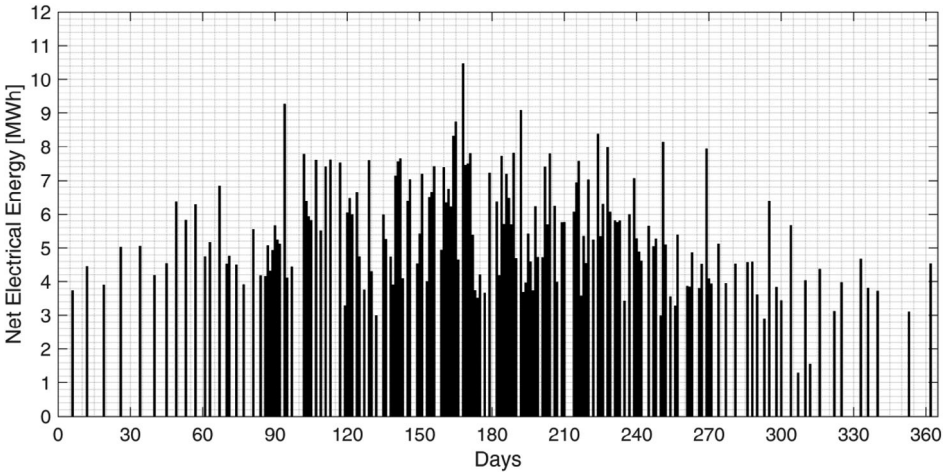

FIGURE 7 Daily net energy production of the ORC unit throughout the year

TABLE 4 Comparison of the expected yearly system performance based on the different TES configurations

	Two-tank system	One-tank thermocline system (Rock + Sand)	One-tank Thermocline (Rock + Sand + PCM)	No TES
Solar energy availability [GWh_t]	16.03	16.03	16.03	16.03
Solar field energy output [GWh_t]	4.86	5.09	5.08	4.81
Defocusing energy losses [GWh_t]	0.01	0.01	0.01	0.15
TES thermal losses [GWh_t]	0.18	0.06	0.06	0
ORC thermal energy input [GWh]	4.68	5.03	5.02	4.81
ORC energy production [GWh]	0.92	0.92	0.92	0.78
Mean ORC efficiency [%]	19.7	18.2	18.3	16.2

4.2 | Yearly analysis

Annual weather and environmental data were obtained for the Ottana site using Meteonorm software,[47] and they form the basis for yearly performance evaluation of the solar plant. Figure 7 shows the daily electricity production during one year of operation in the case of the one-tank configuration filled with rock and sand. A very similar distribution of the daily electrical energy production is obtained with the other two TES configurations analysed due to the similar storage capacity. As expected, most of the annual electricity production is concentrated during summer, when daily energy production over 10 MWh is reached, while during winter the ORC unit is operative only one day per week on average.

Table 4 reports the main performance indexes of the two proposed configurations compared to the actual one with two-tank direct TES and with the CSP-ORC plant without any TES system. The latter is taken as a reference for assessing the energy benefit arising from the inclusion of an energy storage system in the considered solar plant. The existing two-tank direct TES case overcomes the instability of the thermal power generated by the solar field. The presence of this TES device raises the ORC mean yearly efficiency up to a value of 19.7% and the ORC electrical energy production up to 0.92 GWh per year. The ORC unit operates only when the hot tank is almost full, providing, therefore, hot oil at a mass flow rate and temperature quite stable close to the nominal values, allowing to raise the main performance indicators.

Since the HTF temperature feeding the ORC unit was observed to be well below the nominal value for the one-tank configuration, it results in a reduction of the mean yearly ORC efficiency, which is about 18.2% when considering the packed-bed TES with silica. The introduction

TABLE 5 Assumptions and results of the preliminary economic assessment for the different TES configurations[49-52]

	Two-tank direct option	One-tank packed-bed option (Rock + Sand)	One-tank packed-bed option (Rock + Sand + PCM)
Vessel volume	330 m^3 × 2	330 m^3	330 m^3
Specific vessel costs	200 €/m^3	200 €/m^3	200 €/m^3
Storage medium content	195 t (HTF)	67 t (HTF) 607 t (Silica)	63 t (HTF) 557 t (Silica) 33 t (PCM)
Specific storage medium costs	2.5 €/kg (HTF)	2.5 €/kg (HTF) 0.15 €/kg (Silica)	2.5 €/kg (HTF) 0.15 €/kg (Silica) 1.0 €/kg (PCM)
Initial costs	0.620 M€	0.325 M€	0.341 M€
LCOS	0.447 €/kWh	0.234 €/kWh	0.246 €/kWh

of a layer with encapsulated PCM ameliorates this drawback but the effect is quite marginal, since the mean ORC efficiency rises only to 18.3%. Conversely, adopting a one-tank system with a lower average temperature strongly reduces the TES thermal losses towards the environment. Furthermore, an increase in the solar field annual production is also observed compared to the two-tank system, since the overall receiver thermal losses are lower.

Consequently, the annual electricity production obtained by the three TES configurations analysed is almost the same (0.92 GWh/year), confirming that the two alternative solutions based on a single tank are a valid alternative to the current two-tank system in use.

4.3 | Preliminary economic analysis

The prospective economic benefit of the alternative TES configurations is assessed in this section. The solar field and ORC unit are already installed, thus, the preliminary economic assessment concerns only the storage units. In view of this, the economic assessment uses levelized cost of storage (LCOS)[48] as a performance index, defined as:

$$\mathrm{LCOS} = \frac{\mathrm{CAPEX_{TES}} + \sum_{k=1}^{N} \frac{\mathrm{OPEX_{TES}}}{(1+r)^k}}{\sum_{k=1}^{N} \frac{E_{CSP+TES} - E_{CSP,only}}{(1+r)^k}} \quad (18)$$

with $\mathrm{CAPEX_{TES}}$ representing the capital expenditures of the TES section, and $\mathrm{OPEX_{TES}}$ the yearly operational expenditures of the TES unit. The expected yearly energy production, $E_{CSP+TES}$, refers to the production of the CSP plant with integrated TES unit, while $E_{CSP,only}$ represents the yearly energy produced by the CSP section only, without any thermal storage device. The interest rate i is taken as 5%, while the TES system lifetime N is taken as 25 years. The $\mathrm{CAPEX_{TES}}$ were arrived at considering the market unit cost of each vessel. Specifically, total capital costs were obtained by adding unit costs for the number of tanks involved, which can be 1 or 2 depending on the chosen TES configuration, added also to the costs of the storage media, proportional to the mass amount of HTF, Silica rock and sand and encapsulated PCM. The yearly operational costs are taken as 3% of the capital costs. The CAPEX would be expected to reduce significantly with the use of the one-tank packed-bed unit, apparently as a result of savings made in the purchase of vessels, as reported in Table 5. Moreover, a more favourable unit cost of the silica compared to thermal oil decreases further the capital investment. Consequently, a reduction of more than 45% in the capital investment costs of TES system is observed with the adoption of a one-tank packed-bed TES, relative to the two-tank alternative. This fact, combined with the equivalent annual energy production obtained irrespective of the TES technology, results in a significant reduction of the achieved LCOS with the adoption of a one-tank TES. In particular, the use of the sole packed bed made by rock and sand gives the lowest LCOS (0.234 €/kWh), while the introduction of a PCM layer seems to provide no economic benefit.

5 | CONCLUSIONS

Performance of different TES configurations have been assessed for medium-scale CSP systems, with reference to a real CSP-ORC plant rated nominally at 629 kW. The CSP-ORC plant currently operates with a two-tank direct TES system using Therminol SP-I as storage medium and HTF. In this paper, the effects on the CSP-ORC plant of a one-tank packed-bed TES using rock and sand as storage media and another similar one with integrated PCM were

comparatively assessed, against the existing two-tank system. The main findings of the study are:

- The use of a one-tank packed bed TES system increased annual thermal energy output of the solar field to about 5.1 GWh_t, around 5% higher than that obtained with the use of the two-tank direct system. Similarly, the study revealed that adoption of a one-tank TES system in the CSP-ORC plant would reduce annual thermal energy loss in the TES system to about one-third of what currently obtains. Consequently, a rise in the annual thermal energy feeding the ORC unit (about 5 GWh_t) is expected with the use of a one-tank system, compared to about 4.7 GWh_t obtainable with the two-tank TES system.
- Overall, about 0.92 GWh of electrical energy is produced by the ORC annually, irrespective of the TES configuration employed. Thus, in juxtaposition with the annual thermal energy input into the ORC reported above for the different TES configurations, it is obtained that adoption of a one-tank TES system reduces mean ORC efficiency by about 1.5% points.
- Lack of constraints in temperature of the oil exiting the one-tank packed bed TES system allowed for a greater amount of thermal energy available to be exploited during the discharging phase. Additionally, this choice had the obvious advantage of canceling the hysteresis effect usually generated after consecutive charge/discharge cycles, that would have degraded the thermocline shape with significant reduction of the thermal energy available for input into the ORC plant.
- The one-tank packed-bed system is economically viable due to the reduced cost of investment. Consequently, a reduction of more than 45% in the levelized cost of storage can be achieved compared to the two-tank configuration, while the integration of a PCM layer seems not to introduce any economic benefit.

In the near future, a further experimental campaign on the CSP plant is scheduled with the aim of increasing the reliability of the simulation models adopted and the robustness of the results obtained in this study.

NOMENCLATURE

A	area (m^2)
c	specific heat (J/kg K)
CAPEX	capital expenditures (€)
E	energy (Wh)
k	thermal conductivity (W/m K)
h	specific enthalpy (J/kg)
L	latent heat (J/kg)
$\dot{m}$	mass flow rate (kg/s)
OPEX	operating expenditures (€/year)
$\dot{Q}$	thermal power (W)
T	temperature (K)
t	time (s)
U	overall heat transfer coeff. (W/m^2 K)
V	volume (m^3)
α	convective heat transfer coeff. (W/m^2 K)
ε	void fraction
η	efficiency
ρ	density (kg/m^3)
AMB	ambient conditions
CLN	cleanliness
CT	cold tank
HT	hot tank
I	inlet side
O	outlet side
OPT	optical
REC	receiver
SF	solar field
CSP	concentrated solar power
DNI	direct normal irradiance
HTF	heat transfer fluid
LCOS	levelized cost of storage
ORC	organic Rankine cycle
PCM	phase change material
TES	thermal energy storage

ACKNOWLEDGEMENTS

The study reported in this paper received funding from P.O.R. SARDEGNA F.S.E. 2014-2020—Axis III Education and Training, Thematic Goal 10, Specific goal 10.5, Action partnership agreement 10.5.12—"Call for funding of research projects—Year 2017." The authors gratefully acknowledge ENAS for granting access to the operational data of the Ottana Solar Facility.

ORCID

Mario Petrollese https://orcid.org/0000-0001-5394-1419

REFERENCES

1. OECD. World Energy Outlook 2018; 2018.
2. Modi A, Bühler F, Andreasen JG, Haglind F. A review of solar energy based heat and power generation systems. *Renew Sustain Energy Rev*. 2017;67:1047-1064. https://doi.org/10.1016/J.RSER.2016.09.075.
3. Bouhal T, Aqachmar Z, Kousksou T, El Rhafiki T, Jamil A, Zeraouli Y. Energy and economic assessment of a solar air-conditioning process for thermal comfort requirements. *Sol Energy*. 2020;208:101-114. https://doi.org/10.1016/j.solener.2020.07.045.
4. Vengadesan E, Senthil R. A review on recent development of thermal performance enhancement methods of fl at plate solar water heater. *Sol Energy*. 2020;206:935-961. https://doi.org/10.1016/j.solener.2020.06.059.

5. Esmaeli H, Roshandel R. Optimal design for solar greenhouses based on climate conditions. *Renew Energy*. 2020;145:1255-1265. https://doi.org/10.1016/j.renene.2019.06.090.
6. Hernández-Callejo L, Gallardo-Saavedra S, Alonso-Gómez V. A review of photovoltaic systems: design, operation and maintenance. *Sol Energy*. 2019;188:426-440. https://doi.org/10.1016/j.solener.2019.06.017.
7. Santos JJCS, Palacio JCE, Reyes AMM, Carvalho M, Freire AJR, Barone MA. Concentrating solar power. *Adv Renew Energies Power Technol*. 2018;1:373-402. https://doi.org/10.1016/B978-0-12-812959-3.00012-5.
8. Răboacă MS, Badea G, Enache A, et al. Concentrating solar power technologies. *Energies*. 2019;12:1048. https://doi.org/10.3390/en12061048.
9. Achkari O, El Fadar A. Latest developments on TES and CSP technologies—energy and environmental issues, applications and research trends. *Appl Therm Eng*. 2020;167:114806. https://doi.org/10.1016/j.applthermaleng.2019.114806.
10. Islam T, Huda N, Abdullah AB, Saidur R. A comprehensive review of state-of-the-art concentrating solar power (CSP) technologies: current status and research trends. *Renew Sustain Energy Rev*. 2018;91:987-1018. https://doi.org/10.1016/j.rser.2018.04.097.
11. Gomez-vidal J, Or E, Kruizenga A, Fern AG, Cabeza LF, Sol A. Mainstreaming commercial CSP systems: A technology review. *Renew Energy*. 2019;140:152-176. https://doi.org/10.1016/j.renene.2019.03.049.
12. Dinter F, Gonzalez DM. Operability, reliability and economic benefits of CSP with thermal energy storage: first year of operation of ANDASOL 3. *Energy Procedia*. 2014;49:2472-2481. https://doi.org/10.1016/j.egypro.2014.03.262.
13. Pacheco JE, Showalter SK, Kolb WJ. Development of a molten-salt thermocline thermal storage system for parabolic trough plants. *J Sol Energy Eng*. 2002;124:153-159. https://doi.org/10.1115/1.1464123.
14. Pelay U, Luo L, Fan Y, Stitou D, Rood M. Thermal energy storage systems for concentrated solar power plants. *Renew Sustain Energy Rev*. 2017;79:82-100. https://doi.org/10.1016/j.rser.2017.03.139.
15. Oyekale J, Heberle F, Petrollese M, Brüggemann D, Cau G. Biomass retrofit for existing solar organic Rankine cycle power plants: conceptual hybridization strategy and techno-economic assessment. *Energ Conver Manage*. 2019;196:831-845. https://doi.org/10.1016/j.enconman.2019.06.064.
16. Oyekale J, Petrollese M, Vittorio T, Cau G. Conceptual design and preliminary analysis of a CSP-biomass organic Rankine cycle plant. 31st Int. Conf. Effic. Cost, Optim. Simul. Environ. Impact Energy Syst. ECOS 2018, Guimaraes; Port; 2018.
17. Enescu D, Chicco G, Porumb R, Seritan G. Thermal energy storage for grid applications: current status and emerging trends. *Energies*. 2020;13:340. https://doi.org/10.3390/en13020340.
18. Reddy KS, Mudgal V, Mallick TK. Review of latent heat thermal energy storage for improved material stability and effective load management. *J Energy Storage*. 2018;15:205-227. https://doi.org/10.1016/J.EST.2017.11.005.
19. Kerskes H. *Chapter 17—thermochemical energy storage. In: Letcher TMBT-SE, editor.* . Oxford: Elsevier; 2016:345-372.
20. Alva G, Liu L, Huang X, Fang G. Thermal energy storage materials and systems for solar energy applications. *Renew Sustain Energy Rev*. 2017;68:693-706. https://doi.org/10.1016/j.rser.2016.10.021.
21. Kuravi S, Trahan J, Goswami DY, Rahman MM, Stefanakos EK. Thermal energy storage technologies and systems for concentrating solar power plants. *Prog Energy Combust Sci*. 2013;39:285-319. https://doi.org/10.1016/j.pecs.2013.02.001.
22. Xu C, Wang Z, He Y, Li X, Bai F. Sensitivity analysis of the numerical study on the thermal performance of a packed-bed molten salt thermocline thermal storage system. *Appl Energy*. 2012;92:65-75. https://doi.org/10.1016/j.apenergy.2011.11.002.
23. Singh H, Saini RP, Saini JS. A review on packed bed solar energy storage systems. *Renew Sustain Energy Rev*. 2010;14:1059-1069. https://doi.org/10.1016/j.rser.2009.10.022.
24. Good P, Zanganeh G, Ambrosetti G, Barbato MC, Pedretti A, Steinfeld A. Towards a commercial parabolic trough CSP system using air as heat transfer fluid. *Energy Procedia*. 2013;49:381-385. https://doi.org/10.1016/j.egypro.2014.03.041.
25. Hoffmann J, Fasquelle T, Goetz V, Py X. A thermocline thermal energy storage system with filler materials for concentrated solar power plants: experimental data and numerical model sensitivity to different experimental tank scales. *Appl Therm Eng*. 2016;100:753-761. https://doi.org/10.1016/j.applthermaleng.2016.01.110.
26. Bruch A, Fourmigue JF, Couturier R, Molina S. Experimental and numerical investigation of stability of packed bed thermal energy storage for CSP power plant. *Energy Procedia*. 2014;49:743-751. https://doi.org/10.1016/j.egypro.2014.03.080.
27. Bruch A, Fourmigué JF, Couturier R. Experimental and numerical investigation of a pilot-scale thermal oil packed bed thermal storage system for CSP power plant. *Sol Energy*. 2014;105:116-125. https://doi.org/10.1016/j.solener.2014.03.019.
28. Couturier R, Bruch A, Molina S, Esence T, Fourmigu JF. Experimental investigation of cycling behaviour of pilot-scale thermal oil packed-bed thermal storage system. *Renew Energy*. 2017;103:277-285. https://doi.org/10.1016/j.renene.2016.11.029.
29. Rodat S, Bavière R, Bruch A, Camus A. Dynamic simulation of a Fresnel solar power plant prototype with thermocline thermal energy storage. *Appl Therm Eng*. 2018;135:483-492. https://doi.org/10.1016/j.applthermaleng.2018.02.083.
30. Rodat S, Bruch A, Dupassieux N, El Mourchid N. Unique Fresnel demonstrator including ORC and thermocline direct thermal storage: operating experience. *Energy Procedia*. 2015;69:1667-1675. https://doi.org/10.1016/j.egypro.2015.03.127.
31. Chacartegui R, Vigna L, Becerra JA, Verda V. Analysis of two heat storage integrations for an organic Rankine cycle parabolic trough solar power plant. *Energ Conver Manage*. 2016;125:353-367. https://doi.org/10.1016/j.enconman.2016.03.067.
32. Rodríguez JM, Sánchez D, Martínez GS, et al. Techno-economic assessment of thermal energy storage solutions for a 1 MWe CSP-ORC power plant. *Sol Energy*. 2016;140:206-218. https://doi.org/10.1016/j.solener.2016.11.007.
33. Galione PA, Pérez-segarra CD, Rodríguez I, Lehmkuhl O, Rigola J. A new thermocline-PCM thermal storage concept for CSP plants . Numerical analysis and perspectives. *Energy Procedia*. 2014;49:790-799. https://doi.org/10.1016/j.egypro.2014.03.086.
34. Galione PA, Pérez-Segarra CD, Rodríguez I, Oliva A, Rigola J. Multi-layered solid-PCM thermocline thermal storage concept for

CSP plants. Numerical analysis and perspectives. *Appl Energy*. 2015;142:337-351. https://doi.org/10.1016/j.apenergy.2014.12.084.

35. Zanganeh G, Commerford M, Haselbacher A, Pedretti A, Steinfeld A. Stabilization of the outflow temperature of a packed-bed thermal energy storage by combining rocks with phase change materials. *Appl Therm Eng*. 2014;70:316-320. https://doi.org/10.1016/j.applthermaleng.2014.05.020.
36. Petrollese M, Cau G, Cocco D. The Ottana solar facility: dispatchable power from small-scale CSP plants based on ORC systems. *Renew Energy*. 2018;147:2932-2943. https://doi.org/10.1016/j.renene.2018.07.013.
37. Therminol SP. Heat Transfer Fluid | Therminol | Eastman; n.d.
38. Cocco D, Migliari L, Petrollese M. A hybrid CSP–CPV system for improving the dispatchability of solar power plants. *Energ Conver Manage*. 2016;114:312-323. https://doi.org/10.1016/j.enconman.2016.02.015.
39. Forristall R. Heat transfer analysis and modeling of a parabolic trough solar receiver implemented in engineering equation solver; 2003.
40. Cocco D, Migliari L, Serra F. Influence of thermal energy losses on the yearly performance of medium size CSP plants. ECOS 2015—28th Int. Conf. Effic. Cost, Optim. Simul. Environ. Impact Energy Syst., 2015.
41. Petrollese M, Cocco D. Techno-economic assessment of hybrid CSP-biogas power plants. *Renew Energy*. 2020;155:420-431. https://doi.org/10.1016/j.renene.2020.03.106.
42. Cascetta M, Cau G, Puddu P, Serra F. A comparison between CFD simulation and experimental investigation of a packed-bed thermal energy storage system. *Appl Therm Eng*. 2016;98:1263-1272. https://doi.org/10.1016/j.applthermaleng.2016.01.019.
43. Cascetta M, Serra F, Arena S, Casti E, Cau G, Puddu P. Experimental and numerical research activity on a packed bed TES system. *Energies*. 2016;9:758. https://doi.org/10.3390/en9090758.
44. Wakao N, Kaguei S. *Heat and Mass Transfer in Packed Beds*. Topics in chemical engineering New York, NY; Gordon and Breach Science Publishers; 1982.
45. Jefferson CP. Prediction of breakthrough curves in packed beds. *AIChE J*. 1972;18:409-420.
46. Petrollese M, Dickes R, Lemort V. Experimentally-validated models for the off-design simulation of a medium-size solar organic Rankine cycle unit. *Energ Conver Manage*. 2020;224:113307. https://doi.org/10.1016/j.enconman.2020.113307.
47. Meteotest. Meteonorm Software—Worldwide irradiation data; n.d.
48. Petrollese M, Arena S, Cascetta M, Casti E, Cau G. Techno-economic comparison of different thermal energy storage technologies for medium-scale CSP plants. *AIP Conf Proc*. 2019;2191:020128. https://doi.org/10.1063/1.5138861.
49. Cocco D, Serra F. Performance comparison of two-tank direct and thermocline thermal energy storage systems for 1MWe class concentrating solar power plants. *Energy*. 2015;81:526-536. https://doi.org/10.1016/j.energy.2014.12.067.
50. Pereira da Cunha J, Eames P. Thermal energy storage for low and medium temperature applications using phase change materials—a review. *Appl Energy*. 2016;177:227-238. https://doi.org/10.1016/j.apenergy.2016.05.097.
51. Gil A, Castell A, Oro E, Cabeza BLF, Sole C. Review of solar thermal storage techniques and associated heat transfer technologies. *Environ Sci*. 2012;100:525-538.
52. Fritsch A, Frantz C, Uhlig R. Techno-economic analysis of solar thermal power plants using liquid sodium as heat transfer fluid. *Sol Energy*. 2019;177:155-162. https://doi.org/10.1016/j.solener.2018.10.005.

How to cite this article: Cascetta M, Petrollese M, Oyekale J, Cau G. Thermocline vs. two-tank direct thermal storage system for concentrating solar power plants: A comparative techno-economic assessment. *Int J Energy Res*. 2021;45(12):17721-17737. https://doi.org/10.1002/er.7005